Rotational and Translational Velocity and Acceleration Thresholds for the Onset of Cybersickness in Virtual Reality

Lorenzo Terenzi* and Peter M. T. Zaal†
San José State University
NASA Ames Research Center
Moffett Field, CA 94035

This paper determined rotational and translational velocity and acceleration thresholds for the onset of cybersickness. Cybersickness causes discomfort and discourages the widespread use of virtual reality systems for both recreational and professional use. Visual motion or optic flow is known to be one of the main causes of cybersickness due to the sensory conflict it creates with the vestibular system. The aim of this experiment is to detect rotational and translational velocity and acceleration thresholds that cause the onset of cybersickness. Participants were exposed to a moving particle field in virtual reality for a few seconds per run. The field moved in different directions (longitudinal, lateral, roll, and yaw), with different velocity profiles (steady and accelerating), and different densities. Using a staircase procedure, that controlled the speed or acceleration of the field, we detected the threshold at which participant started to feel temporary symptoms of cybersickness. The optic flow was quantified for each motion type and by modifying the number of features, the same amount of optic flow was present in each scene. Having the same optic flow in each scene allows a direct comparison of the thresholds. The results show that the velocity and acceleration thresholds for rotational optic flow were significantly lower than for translational optic flow. The thresholds suggestively decreased with the decreasing particle density of the scene. Finally, it was found that all the rotational and translational thresholds strongly correlate with each other. While the mean values of the thresholds could be used as guidelines to develop virtual reality applications, the high variability between individuals implies that the individual tuning of motion controls would be more effective to reduce cybersickness while minimizing the impact on the experience of immersion.

I. Nomenclature

OF	=	Optic Flow, pixels s^{-1}
I	=	Pixel brightness intensity
v_s	=	Screen speed, pixels s^{-1}
s_p	=	Physical diameter of the particle, m
d	=	Distance from observer in 3D space, m
r	=	Radial distance from observer, m
$r_{\alpha p}$	=	Angular size of a pixel rad^{-1}
$v_\perp$	=	Velocity perpendicular to the raycast from the observer, m s^{-1}
h	=	Length of the particle field, m
n	=	Number of particles
ρ	=	Particle density, m^{-3}
α	=	Half of the angular field of view, rad
α	=	Angular acceleration, rad s^{-2}
a	=	Linear Acceleration, m s^{-2}
V_t	=	Mean velocity threshold for translations, m/s
ω_t	=	Mean angular velocity threshold for rotations, rad/s

*Research Scholar, Human Systems Integration Division, Mail Stop 262-2, lorenzo.terenzi@nasa.gov.
†Senior Research Engineer, Human Systems Integration Division, Mail Stop 262-2, peter.m.t.zaal@nasa.gov, Senior Member.

V_{vec} = Perceived velocity, m s^{-1}
ω_{vac} = Perceived angular velocity, rad s^{-1}
V_z = Forward velocity, m s^{-1}
V_x = Lateral velocity, m s^{-1}
ω_{roll} = Angular velocity around roll axis, rad s^{-1}
ω_{yaw} = Angular velocity around yaw axis, rad s^{-1}
τ_r = Time constant for rotational low pass filter, s
τ_t = Time constant for translations' low pass filter, s
s = Laplace variable, s^{-1}

II. Introduction

This paper examines the rotational and translational velocity and acceleration thresholds for the onset of cybersickness. Cybersickness is experienced by many users of virtual reality (VR) applications. Previous studies have linked optic flow or vection to cybersickness. However, no consensus exists on the type and intensity of optic flow that induces cybersickness. In particular, both stationary optic flow, i.e., with constant velocity, and accelerating optic flow have been argued to be triggers. In addition, both rotations and translations have been found to induce sickness. A better understanding of the effects of different types of optic flow on cybersickness can help the development of methods to reduce it, such as dynamic modification of the field of view in VR [1].

Limited research has been devoted to understanding the origins of cybersickness in VR. Increasing the rotational rate of visual inputs has been shown to increase the symptoms of cybersickness [2, 3]. It has also been shown that rotations around multiple axes are more sickening than those around one axis [4]. On the other hand, current developers of VR games suggest that reducing accelerations by providing an observer with an instantaneous acceleration to the correct speed will help to reduce cybersickness [5, 6]. These recommendations, mostly aimed at prospective VR developers, are not backed by strong evidence, even though it has been shown that an accelerating observer seems to experience more motion sickness using conventional displays [7]. Finally, jittering or a series of high-frequency accelerations of the visual field have been shown to induce strong motion sickness as well.

This paper presents an experiment in which participants experienced different types of optic flow in VR with constant velocities or constant accelerations. In each condition, a staircase procedure was followed to find the threshold for the onset of cybersickness. Note that cybersickness develops over time; that is, symptoms increase when certain conditions persist. This experiment focused on the onset of cybersickness when symptoms first start to appear. The associated symptoms also often disappear in a very short span of time.

III. Method

In this section, we present the research methodology of the experiment. In subsection III.A we present the current state of the art of the understanding of cybersickness and recommended ways to mitigate it. In subsection III.B we give an overview of optic flow and in subsection III.C we show how we model and compute the optic flow for different experimental conditions. Furthermore, in subsection III.D we give a precise description of the task used in the experiment.

A. Background

Currently, the most accredited theory to explain part of the origin of cybersickness is the theory of sensory mismatch despite the existence of alternative theories, such as the "Postural Instability" and "Rest Frame" theories [8]. In this article, we only considered the sensory mismatch theory, which predicts the occurring of motion sickness whenever there is a mismatch mainly between the expected motion from the visual system and the vestibular system.

Cybersickness can be caused by many factors, including a rendering lag, screen brightness, focal distance, jittering, scene motion, etc. This paper focused on investigating the role of optic flow, which is caused by motion in the virtual scene. It has been shown that motion in the virtual scene can be nauseogenic [9]. Indeed, what seems to increase or generate simulator sickness in VR is vection, i.e, the sensation of self-motion induced via a visual stimulus [7]. VR systems are particularly prone to generate vection due to the strong immersion that the user can experience in the virtual world. A recent review has shown that the level of immersion or presence in VR is correlated with the level of cybersickness that participants experienced [10]. Another study showed that increased fidelity and details in the scene,

which lead to increased presence and optic flow, also leads to a greater chance of experiencing motion sickness [11]. Cybersickness is frequently measured through the simulator sickness questionnaire (SSQ), through which the symptoms are further sub-classified in nausea, oculomotor related and disorientation [8].

Current solutions to minimize the chances of cybersickness are either technical solutions or recommendations aimed at VR software developers . Currently considered technical solutions are dynamic camera focus, made possible with the use of an eye tracker [6], dynamic changes of the size of the field of view [1], and blurring of non-salient areas in the scene [12]. In general, all these methods aim to reduce the amount of optic flow, in particular in the peripheral vision, while trying to minimize the reduction of immersion of the user. Several recommendations for software developers can be found in the Oculus guide [5]. Some of these recommendations suggest avoiding accelerations, moving at a walking pace, and reducing the motion in the scene not caused by the movement of the user. While these recommendations are extremely valuable, often they are based on anecdotal evidence or feedback from the users. With our research, we are both trying to understand the basic variables that control the onset of cybersickness and at the same time verify and develop guidelines for developers that be can be used to design the motion type and speed in a VR application. Having a more complete understanding of the underlying optic flow variables that play a role can help to guide future research aimed at finding technical solutions for cybersickness.

B. Optic Flow

Optic flow can be defined as the apparent motion of brightness features in an image [13]. The concept of optic flow was developed in the 1940s by Gibson who realized that animals also make use of optic flow to determine their position and velocity in space [14]. For example, bees use optic flow to control their velocity and attitude while landing [15]. Optic flow is also critically important for humans, for everyday tasks, but also for manually controlling moving vehicles. Humans use optic flow to infer their relative velocity and direction in the environment [16–18]. There are many methods to estimate the motion of the observer from the optic flow, of which the most common and traditionally used is the Lucas-Kanade method [19]. Optic flow can also be thought of as a vector field and many methods to quantify it rely on this intuition. Each uniform optic flow field can be decomposed in six basic vector fields that are the six degrees of freedom in 3D space corresponding to translation and rotations around the three axis.

In our experiment, we exposed participants to translating and rotating visual fields to detect the velocity and acceleration thresholds at which the onset of cybersickness appears. It is not clear though, how to compare the different thresholds, each with different units, to each other. To resolve this problem we made use of the concept of optic flow. We opted for a very simple visual field, made of bright moving particles on a black background. The simplicity of the scenarios allowed us to model analytically the optic flow across the different scenes and ensure that all the visual motion conditions had the same amount of optic flow. For our experiment, we only considered four types of motion: longitudinal and lateral translations, and roll and yaw rotations. Vertical translations and pitch rotations were excluded because they are more uncommon movements in VR and their movement properties are similar to lateral translations and roll rotations, respectively.

C. Optic Flow Model

To ensure that the optic flow experienced by the user was the same across conditions we had to find a way of quantifying it. In this section, we derive a simplified formula for calculating the optic flow of for the 4 different optic flow types. The following assumptions were used:

1) Particles when projected onto the head-mounted display (HMD) do not overlap. This assumption is mostly true due to the relative sparsity of the particles in 3D space.
2) We assumed time is continuous. The simulation is always above 60 Hz and motion is perceived as continuous by the user.
3) Particles are sparse enough such the probability that a pixel is occupied by a particle for two consecutive frames is negligible.
4) Particle brightness is constant over time.
5) The field of view (FOV) is assumed to be a cone emanating from the observer as shown in Fig. 2.

We quantified the optic flow by multiplying the intensity of the pixels by their screen velocity:

$$OF = \sum_{x=0,y=0}^{N_x,N_y} I(x,y)v(x,y) = \sum_{i=0}^{N} s_{p_i} v_{s_i} \tag{1}$$

where the sum over all the pixels was converted to a sum over all the particles by normalizing the brightness $I(x, y)$ from 0 (black) to 1 (white). s_{p_i} stands for the size of the particles in units of pixels and v_i it's apparent velocity on the screen in pixels per second. The equation can be further expanded since the particle size in pixels is related to its angular size $s_p = r_{\alpha p} s_\alpha$ where $r_{\alpha p}$ is the number of pixels per radians of field of view. We can express the angular size of the particle in terms of its real size to obtain:

$$OF = s r_{\alpha p} \sum_{i=0}^{N} \frac{v_{si}}{d_i} \tag{2}$$

where d_i is the distance of the i$^{\text{th}}$ particle from the observer and s is the particle size in physical units. The s variable has be taken out of the summation since it's constant for all particles. To express the optic flow OF as a function of the particle field velocity we used cylindrical coordinates as can be seen in Fig. 1.

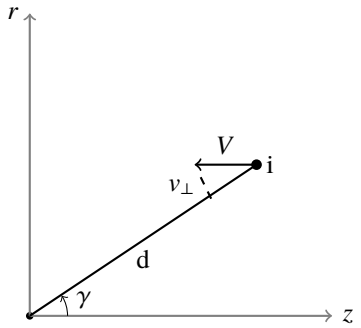

Fig. 1 A particle i moving towards an observer.

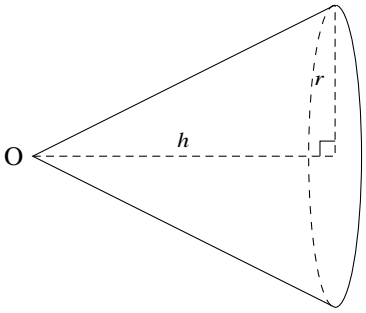

Fig. 2 Field of view representation.

In this subsection we will derive the expression for the forward moving scene and provide the final equations only for the other three scene motion types. We first expressed Eq. 2 in terms of physical linear or angular velocities and the particle density of the field. For the forward translational motion case, the screen velocity v_{si} can be expressed as:

$$v_{si} = v_{\alpha_i} r_{\alpha p} = r_{\alpha p} \frac{v_\perp}{d_i} = r_{\alpha p} \frac{V \sin\gamma}{d_i} = r_{\alpha p} \frac{V r_i}{d_i^2} \tag{3}$$

where v_α is the angular velocity of the particle on the screen, $v_\perp$ is the velocity perpendicular to the ray connecting the particle and the observer, V is the uniform absolute velocity of the field, r_i is the radial distance of particle i from the observer, and d_i is the distance from the observer. A diagram of the moving particle i is shown in Fig. 1. Substituting the equation of v_{si} into the equation for optic flow we obtain:

$$OF_z = r_\alpha^2 s V \sum \frac{r_i}{{d_i}^3} \tag{4}$$

To simplify the expression we take the mean value of the optic flow:

$$\overline{OF_z} = r_\alpha^2 s V n \, \mathrm{E}\left(\frac{r}{d^3}\right) \tag{5}$$

where n is the number of particles and E is the expectation operator. We can express the mean as an integral over the conic volume, representing the field of view, such that $r = \tan\alpha z$, where α is half the field of view and z is the height of the cone which ranges from 0 to 2. Assuming that the particles are uniformly distributed, we can find a numerical value for the mean optic flow by expressing the expectation operator as a volume integral:

$$\overline{OF}_z = 2\pi\rho_z r_\alpha^2 s V_z \int_0^h \int_0^{z\tan\alpha} \frac{r}{\left(r^2+z^2\right)^{\frac{3}{2}}} dr dz = 2\pi\rho_z r_\alpha^2 s V_z I_z \tag{6}$$

where I_z is the numerical value of the integral. Similarly, for lateral translational motion, the mean optic flow is:

$$\overline{OF}_x = 2\pi\rho_x r_\alpha^2 s V_x \int_0^h \int_0^{z\tan\alpha} \frac{z}{\left(r^2+z^2\right)^{\frac{3}{2}}} dr dz = 2\pi\rho_x r_\alpha^2 s V_x I_x \tag{7}$$

For the rotational cases, the derivation is very similar and we obtain for yaw rotations:

$$\overline{OF}_{yaw} = 2\pi\rho_{yaw}r_{\alpha}^{2}s\omega_{yaw}\int_{0}^{h}\int_{0}^{z\tan\alpha}\frac{z}{r^{2}+z^{2}}drdz = 2\pi\rho_{yaw}r_{\alpha}^{2}s\omega_{yaw}I_{yaw} \tag{8}$$

where ω_{yaw} is the yaw rotation rate of the field in rad s^{-1}. For roll rotations, the expression for the mean of optic flow is:

$$\overline{OF}_{roll} = 2\pi\rho_{roll}r_{\alpha}^{2}s\omega_{roll}\int_{0}^{h}\int_{0}^{z\tan\alpha}\frac{r}{r^{2}+z^{2}}drdz = 2\pi\rho_{roll}r_{\alpha}^{2}s\omega_{roll}I_{roll} \tag{9}$$

All the optic flow values are proportional to $2\pi\rho r_{\alpha}^{2}s$. This implies that OF is linear w.r.t. the density ρ and the particle size s, and increases quadratically with the resolution of the HMD. The distance of a moving particle from the observer was expressed as $d = \sqrt{z^2 + r^2}$. Thus, the optic flow attributed to rotations is approximately inversely proportional to the distance of the particles while the optic flow due to translations to the inverse of the square of the distance.

We expressed each velocity variable in terms of the initial velocity, set at the beginning of the run, times a multiplier that is changed by the staircase procedure. For example $V_z = k_z V_{z0}$, where k_z at the end of the run is equal to the detected threshold. Furthermore, since all conditions start with the same numerical values for the velocity, $\|V_{z0}\| = \|V_{x0}\| = \|\omega_{yaw}\| = \|\omega_{roll}\| = 0.1$. To ensure an equal amount of initial optic flow across different scenes, we enforced that $\|OF_{x-0}\| = \|OF_{z-0}\| = \|OF_{yaw-0}\| = \|OF_{roll-0}\|$. This implied that $\|\rho_x I_x\| = \|\rho_z I_z\| = \|\rho_{yaw} I_{yaw}\| = \|\rho_{roll} I_{roll}\|$. Therefore, we chose to scale all the densities w.r.t. density of the forward translational condition. The density ratios for each optic flow type are provided in Table 1.

Table 1 List of the density ratios for the different scenes.

Optic Flow	OF_z	OF_x	OF_{roll}	OF_{yaw}
$\frac{\rho_i}{\rho_z}$	1	0.54	0.60	0.33

D. Task

Velocity and acceleration thresholds were determined using a staircase procedure [20, 21]. Using this procedure, the value of the velocities or accelerations was gradually increased each run until subjects felt uneasy. Once the initial threshold was detected, the algorithm converged by progressively reducing the change in velocity or acceleration between successive conditions until the desired precision is reached.

Participants used an HMD to enter a VR environment. In the virtual environment, participants were first exposed to a countdown with a red dot in the center. The participant was asked to look in the direction of the red dot for the entire duration of the run (5-3 s). After 3 s the countdown disappeared and participants were exposed to the moving particle field. The exposure time was 3 seconds for accelerating motion and 5 seconds for constant velocity motion. After the exposure to the field, participants were teleported to a new scene where they were asked whether they felt "uneasy" during the previous run. Participants answered "yes" or "no" through a 3D user interface by using a VR hand controller. They were also reminded to wait before continuing or take a break if they felt any lingering cybersickness symptoms from the previous run. The user interface that was used to report uneasiness is shown in Fig. 3.

IV. Experimental Setup

A. Independent Variables

Three independent variables were used in the experiment: optic flow type with four levels (longitudinal, lateral, roll, or yaw, as visualized in Fig. 4), motion type with two levels (constant velocity or constant acceleration), and density with three levels (the initial density multiplied by the factor 1.00, 0.75 or 0.50).

A full-factorial design with the optic-flow type and the motion type was used resulting in eight experimental conditions. These conditions all had a density factor of 1.00. In addition, two extra conditions were tested for the longitudinally moving optic flow with a density factor equal to 0.75 and 0.50. All independent variables were repeated-measures variables. A Latin square was used to generate the order of the conditions. Table 2 provides the label

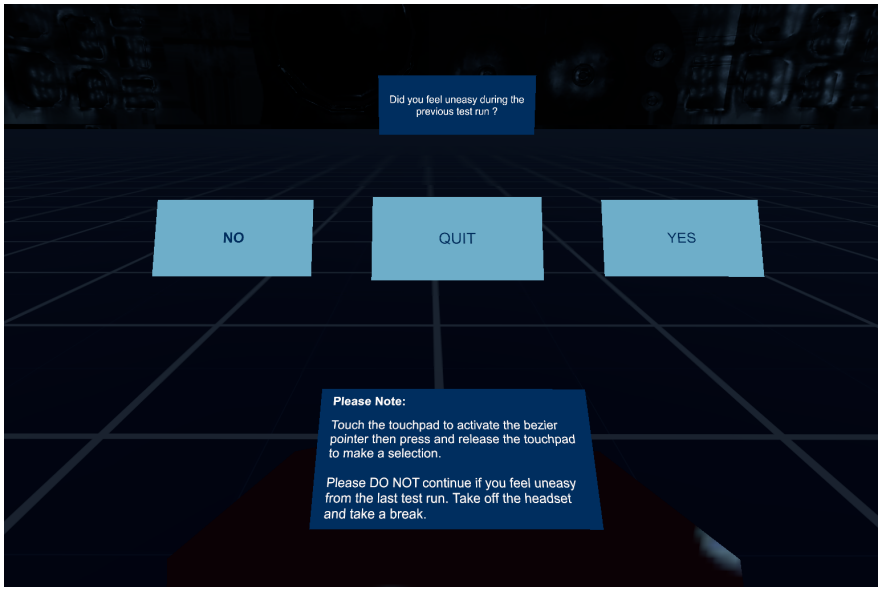

Fig. 3 Virtual user interface that participants used to report uneasiness.

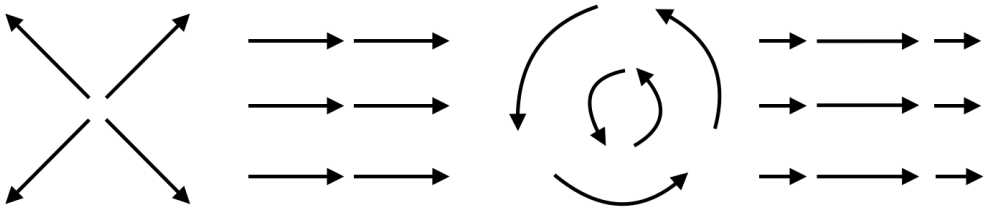

Fig. 4 Optic flow types.

for each experimental condition and the associated independent variables. The label was created by taking the first letter of the optic-flow type and motion type.

Table 2 Experimental conditions.

Independent	Condition Label									
Variable	FS	FA	LS	LA	RS	RA	YS	YA	FS.75	FS.50
Optic Flow	Forward	Forward	Lateral	Lateral	Roll	Roll	Yaw	Yaw	Forward	Forward
Motion	Steady	Acc.	Steady	Acc.	Steady	Acc.	Steady	Acc.	Steady	Steady
Density Factor	1.00	1.00	1.00	1.00	1.00	1.00	1.00	1.00	0.75	0.50

B. Apparatus

The VR hardware equipment consisted of the HTC Vive Pro HMD, two tracking cameras, and one hand controller. The virtual environment was developed with Unity.

Several biometric signals were recorded to see if they could reliably predict the onset of cybersickness [3, 22]. The MindWare Mobile Impedance Cardiograph was used to measure electrocardiogram (ECG) and skin conductivity (GSC).

C. Virtual Environment

The virtual environment consisted in a moving 3D particle field and a scene where participants were asked about their perceived cybersickness onset symptoms. We chose the particle field to elicit vection for its simplicity, which

Fig. 5 VR equipment.

allowed us to explicitly calculate the optic flow and control its underlying variables, such as velocity and density. The field would either translate longitudinally or laterally, or rotate around the roll or yaw axes. The optic-flow field had either a constant velocity or a constant acceleration.

The exposure time to the field was 3 s for accelerating conditions and 5 s for steady conditions. The exposure time was limited since it is one of the main factors that contributes to the severity of cybersickness and we wanted to eliminate it as a confounding variable. During test runs with multiple participants in the design phase of the experiment, we found that 3- and 5-s runs were sufficient to elicit symptoms. The particle field was designed to fill the entire field of view up to a distance of 2 m in front of the observer. The HMD had a field of view of 110 deg. The size of the particles was chosen such that at a distance of 2 m a particle would occupy exactly one pixel of the HMD. The rendering of the scene was always above 60 Hz.

D. Procedures

Participants were briefed about the goal of the experiment. The risks of the experiment were discussed with participants to get their informed consent for participating. Demographics information, their level of experience with VR, and propensity to motion sickness were collected as well.

Participants were informed of all the possible optic-flow types and that it was important to keep their head fixed in a single position and orientation (fix on the red dot present during the countdown, even after it disappeared) at all times as eye movements could be a significant confounding factor for the experiment [23]. The participants had to report if they felt uneasy after each run. Being uneasy was further explained in terms of possible symptoms that could be experienced:

- Vection, i.e., the physical sensation of motion.
- Disorientation, change of sense of vertical, or loss of equilibrium.
- General discomfort and uneasiness.
- Nausea.

Every participant performed all conditions twice, for a total of 20 runs. Before and after performing the first set of conditions, participants had to complete an SSQ. Before the start of the first condition, participants wore the VR headset to familiarize themselves with the scenery and with the user interface used to report the presence of uneasiness. Once the measurements for a particular condition started, each participant had to observe the optic flow in a sequence or trials with different velocities or accelerations according to the staircase procedure. Each trial lasted several seconds and participants indicated if they experienced any discomfort after each trial. Following each answer, the magnitude of the velocity or accelerations in the next run were updated by either subtracting or adding half of the previous step size. When all symptoms of cybersickness disappeared, participants moved onward to the next trial by pressing a button. The staircase ended when the step size reached one-sixteenth of the initial step size. If the participants didn't feel any of the symptoms after 15 steps, they could choose to quit the condition. The order of the conditions was balanced and randomized to ensure that learning/adaptation effects were minimized.

E. Participants

Eighteen participants participated in the experiment. The only requirements set for recruiting were standard VR safety-requirements since some people might be susceptible to seizures or other problems when exposed to VR. The participants had a median age of 24 years (IQR = 27-22). Eleven participants were male and six female. We asked the participants to report their VR experience level and propensity to motion sickness. Nine participants had no VR experience, eight had a low level (1-10 h) of experience. Four participants reported to not be affected by motion sickness, nine to be slightly affected, three to be moderately affected and one to be highly affected.

F. Dependent Measures

The following dependent measures were considered:

- SSQ data, which measured the level of simulator sickness experienced by the subject [24].
- The detected velocity or acceleration thresholds which corresponded to the velocity or acceleration of the optic-flow field (in terms of the multiplier) when the staircase procedure converged.
- Electrocardiogram and skin conductivity, biometrics data that has been shown to correlate with motion sickness [25].

G. Hypotheses

Based on the literature about sensory conflict and the properties of the VR headset we developed the following hypotheses:

$H1$: Rotational conditions were expected to have lower thresholds compared to the translation conditions. Rotational velocities are detected by semicircular canals. The lack of inputs from the vestibular system generates sensory conflict.

$H2$: The threshold for the roll conditions was expected to be lower than the one for the yaw conditions since rolling changes the vertical direction (and therefore the gravity vector) which normally results in the otholits also providing an output in addition to the semicircular canals.

$H3$: For the forward cases, a lower density was expected to result in a higher threshold as the optic flow is directly proportional to the particle field density.

V. Results

A. Missed Detection

Studying the onset of cybersickness is particularly difficult due to the level of intensity of the symptoms. The symptoms are often brief and low in intensity. It was therefore not possible to measure all the thresholds for the ten considered scenarios for each participant.

In Table 3, the number of successful threshold detections per participant are shown. Participant number 14 and 19 have a single missing value due to a technical problem. Participant number 19 could only be tested for each condition once due to logistical constraints. All the other missed detections were caused by the participant not experiencing any symptoms.

Table 3 Number of threshold detections per participant out of a total of 20.

Participant ID	0	1	3	4	5	7	8	9	10	11	13	14	15	16	17	18	19
Num. Runs	20	20	20	0	18	20	20	13	7	1	5	19	20	20	17	20	9

B. Effect of Motion

A summary of the detected threshold values for each optic-flow type and motion type is provided in Table 4. As can be seen, the sample standard deviation is relatively high compared to the mean indicating high individual variability. Figs. 6 and 7 show the error bar plots of the measured velocity and acceleration thresholds with 95 % confidence intervals corrected for within subject variability.

Table 4 Mean and standard deviation of the thresholds across conditions.

Label	Motion	Threshold Mean	Threshold Std
FS	steady	1.183	0.836
LS	steady	0.890	0.594
RS	steady	0.364	0.201
YS	steady	0.473	0.381
FA	accelerating	0.700	0.481
LA	accelerating	0.586	0.417
RA	accelerating	0.474	0.453
YA	accelerating	0.478	0.334

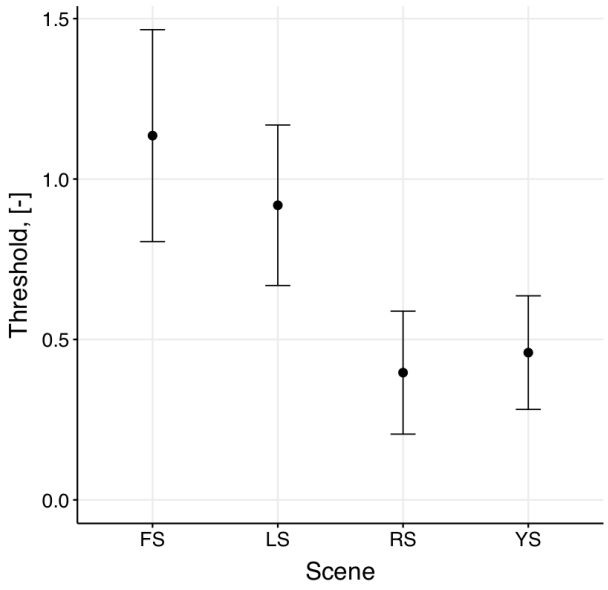

Fig. 6 Constant velocity thresholds.

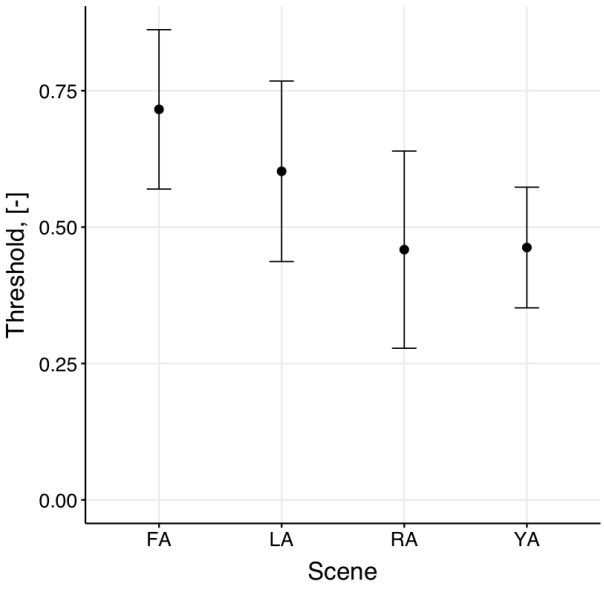

Fig. 7 Constant acceleration thresholds.

For hypothesis testing, a statistical analysis was performed on the threshold data. A simple repeated-measures ANOVA could not be used since the data violated the homogeneity of variances across motion types. We opted to fit a mixed-effect model, first with optic flow type and velocity profile as fixed effects and the participant number as the only random effect. Since the residuals of the model resulted in a skewed normal distribution, the data was log-transformed. Adding a random slope and intercept w.r.t. the motion type or velocity did not significantly improve the model fit. The final model has an Akaike Information Criterion of $AIC = 227.78$ when fit using a maximum likelihood optimizer. To compare the conditions without correcting for multiple comparisons, orthogonal constants were used. The orthogonal contrasts considered were:

- *Translation vs. Rotational*: compares the thresholds for the cases where the particle field translated w.r.t. the cases in which it rotated.
- *Forward vs. Lateral*: compares the thresholds of the forward and lateral moving cases.
- *Roll vs. Yaw*: compares the thresholds of the rolling and yawing cases.

Tables 5 and 6 summarize the results of the statistical tests for the constant velocity and acceleration thresholds.

The detected mean threshold for transnational motion in the constant velocity scenes, $M = 1.035$, was significantly lower than the one for the rotational motion, $M = 0.415$, $b = 0.310(SE = 0.055), t(37.865) = 5.653, p < 0.001$. The other two contrasts, "Forward vs. Lateral" and "Roll vs. Yaw", failed to capture significant trends. Very similar results were found in the scenes with constant acceleration. The mean threshold for translational motion, $M = 0.715$, was significantly

Table 5 Mixed-effect model results of the detected thresholds for steady velocity scenes.

	Estimate	Std. Error	df	t value	p
Translation vs Rotation	0.310	0.055	37.865	5.653	< 0.001
Forward vs Lateral	0.112	0.080	35.916	1.403	0.169
Roll vs Yaw	-0.045	0.072	36.297	-0.630	0.533

= significant ($p < 0.05$)
= suggestive ($0.05 < p < 0.1$)

Table 6 Mixed-effect model results of the detected thresholds for scenes with constant acceleration.

	Estimate	Std. Error	df	t value	p
Translation vs Rotation	0.096	0.038	37.412	2.497	0.017
Forward vs Lateral	0.050	0.054	36.752	0.927	0.360
Roll vs Yaw	-0.004	0.052	36.752	-0.068	0.946

= significant ($p < 0.05$)
= suggestive ($0.05 < p < 0.1$)

lower than the one for the rotational motion, $M = 0.476$, $b = 0.310(SE = 0.055), t(37.865) = 5.653, p < 0.001$. The other two contrasts, "Forward vs. Lateral" and "Roll vs. Yaw", failed to capture significant trends.

C. Effect of Density

Three different densities were tested in the forward-moving scene, with the density scaled by factors 0.50, 0.75 and 1.00. The error-bar plot of the detected thresholds for different densities is provided in Fig. 8. To test whether the threshold was significantly different for different densities, we used mixed-effect models with the subject ID as a random intercept. Mixed-effects models are particularly suited since the dataset was unbalanced due to missing conditions. By fitting the model a suggestive trend was detected. The velocity threshold scaled with the density with a coefficient of $b = -0.411(SE = 0.209)$, $t(23.296) = -1.916$, $p = 0.0619$.

D. SSQ

SSQ data were collected to assess if participants experienced cybersickness symptoms that lasted longer than the single experimental runs. Fig. 9 shows the individual scores for the different symptoms. The total average SSQ score was 3.36 ($CI = 3.52$), which is very low and confirms that sickness symptoms didn't significantly carry over across conditions. Even though the score is very low, a simple t-test revealed that the SSQ scores were only suggestively higher than 0, t(29) = 0.06. The SSQ symptom with the highest score was oculomotor disturbance while nausea had the lowest.

E. Correlation of Conditions

A correlation analysis was used to check whether the thresholds for different conditions were related to each other. We used Pearson's R coefficient as a measure of the correlation between the different conditions. In Fig. 10, the correlation matrix for all the experimental conditions is shown. The conditions are ordered and clustered through a Hierarchical Cluster Analysis [26] to better highlight clusters in the matrix.

The exact correlation coefficient is reported in each square. The white squares indicate that the correlation was not significant, i.e., $p > 0.05$. As can be observed, there were two main correlation clusters: the conditions with translational optic flow (FS, FA, LS, LA, $FS.75$, $FS.50$) strongly correlate with each other and the same holds for conditions with rotatinal optic flow (RS, RA, YS, YA).

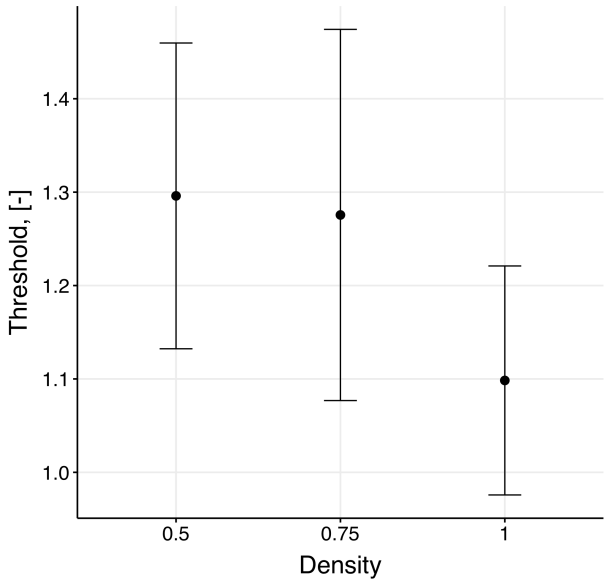

Fig. 8 Thresholds values for different densities.

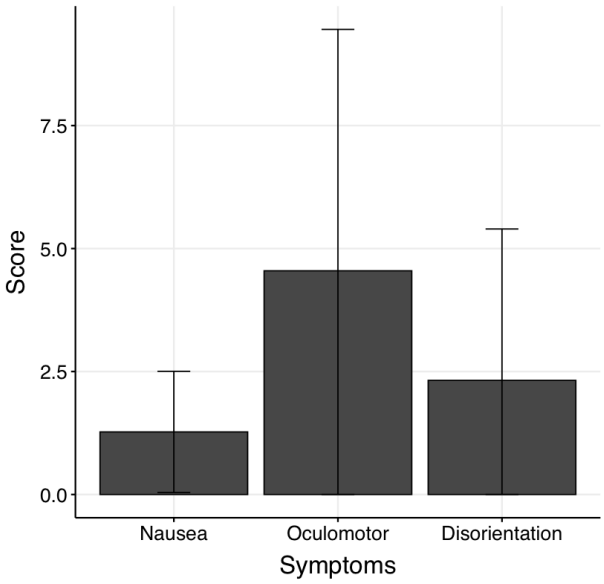

Fig. 9 SSQ scores subdivided by symptoms.

F. Biometrics

The electrocardiogram (ECG) and skin conductivity (GSC) were measured during the experimental runs at a sampling rate of 500 Hz. The measurements were first averaged on a 3 second time window. For the statistical analysis the last three seconds of each run and the the next three seconds after the run's end were considered.

A mixed effect model was fitted to the data with as fixed effect a Boolean representing if participants felt uneasy during the run, and as random effect the participant identifier. The ECG was significantly higher for the runs where participants felt uneasy, $b = 0.118(SE = 0.053)$, $t(3000) = 2.228$, $p = 0.026$. However, as can be seen from the regression coefficient, the effect size was rather small. The GSC did not result significantly different across conditions.

VI. Discussion

In this section we discuss results presented in Sec. V. In subsection VI.B, we focus on the effects of the scene type, in subsection VI.E, on the effects of optic flow densities, and in subsection VI.F, on the correlations between conditions.

A. Role of Optic Flow

Our results indicate that participants' responses to the visual stimuli had a large spread, as can be seen in Table 4. Defining guidelines to avoid cybersickness or quantifying motion characteristics that could lead to cybersickness is particularly hard due to this high variability between individuals. Furthermore, adding to the variability are the varying levels of details of different VR scenes, the number of objects, and different motions of the observer. While we cannot address individual variability, we propose that quantifying the motion in a scene with optic flow can lead to the generalization of experimental findings. Optic flow in complex scenes can be quantified by feature-detection methods like the Lucas-Kanade method [19] and can be used to meaningfully compare different type of motion and scenes. This local approach of feature detection reflects as well the way in which humans perceive motion. Human motion is believed to be perceived through directional selective retinal ganglion cells, which are activated when elementary geometric patterns move in a specified direction [27]. Most of the methods of optic flow estimation also rely on the assumption of constant brightness in the scene, while this assumption might not be necessarily true in practice, it has been shown that retinal ganglion cells are not activated by changes in brightness [28]. Research is needed to verify and possibly find a systematic way of determining the optic flow in different scenes.

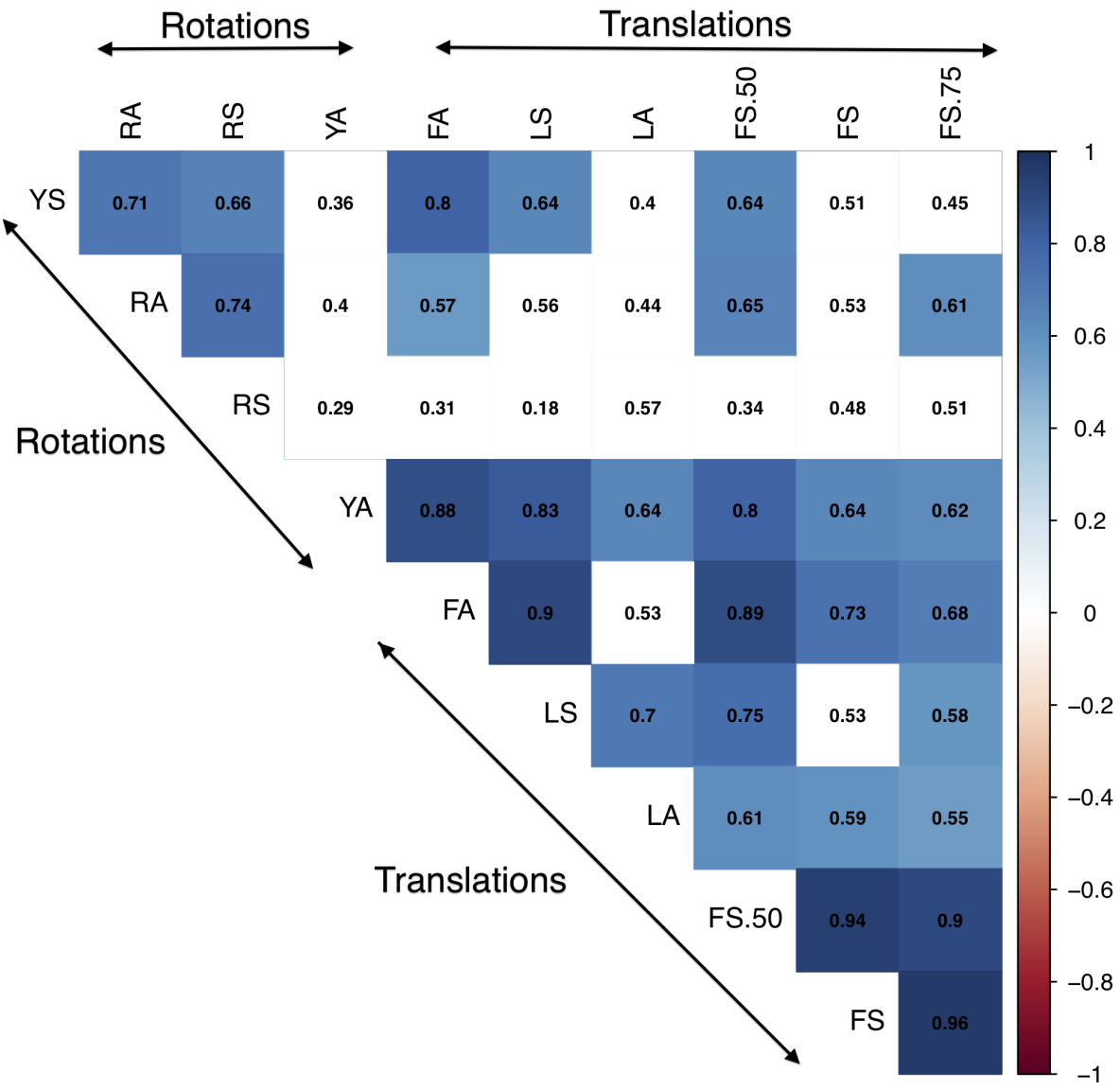

Fig. 10 Person Correlation matrix between the scenarios.

B. Effect of Optic Flow Type

Figs. 6 and 7 show that the type of optic flow, i.e., translations or rotations, significantly impacts the detected thresholds. Conditions with rotations have a lower velocity or acceleration threshold. For example, the forward steady condition had a average velocity threshold, in physical units, of approximately 1.2 m s^{-1}, which is close to walking speed. Oculus recommended a similar forward motion as the most comfortable for users [5]. While it could be just a coincidence, the particle field that surrounded the participant was representative of the amount of optic flow that we experience while walking on a surface in a feature rich environment. On the other hand, a sustained roll rotation of 20 degrees per second is sufficient to induce uneasiness. Even though the physical units are different, we claim that by ensuring the same amount of optic flow for the different scenes given the same speed multiplier, we can sensibly compare the thresholds. The lower amount of optic flow needed to induce uneasiness in the rotational cases is in line with the prediction of the sensory conflict theory. For the steady transnational case, there is, theoretically, no conflict

between the visual system and the vestibular system, since the later one can only detect accelerations. Nonetheless, it is not clear if the visual system perceives an acceleration when a stationary visual field starts moving at a constant speed (which corresponds to an impulse acceleration). On the other hand, the vestibular system can sense (for a short time) constant angular velocities. This implies that, when the visual system perceived rotation in conditions *RS*, *RA*, *YS*, and *YA*, sensory conflict happened. This could contribute to the lower optic flow threshold that was measured. Given the current data, we verified *H1* by showing that velocity and acceleration threshold for rotational optic flow are significantly lower than those for translational optic flow.

The contrast "Roll vs. Yaw" failed to detect any significant differences. This indicates that changing the direction of the rotation did not affect the onset of cybersickness. This extrasensory conflict, as before, seemed to not lower the detected optic flow threshold for the roll condition. This means that we fail to verify *H2*.

C. Effect of Acceleration

The role of the accelerations is hard to analyze because it is difficult to separate its effect on vection and motion sickness from changing velocities, induced by the accelerations themselves. The analysis is complicated by the limited exposure times as well, as for the acceleration scenes it was reduced from 5 to 3 s to avoid reaching very high velocities. Furthermore, the literature on the topic is not aligned. It has been reported that changes in vection or accelerations increase user discomfort and simulator sickness symptoms [5, 7]. On the other hand, traditional studies on human perception and modeling found that accelerations are harder to detect visually and do not contribute to the perception of vection [29–31]. Furthermore, it's not clear if the previous findings are applicable for only a specific frequency band that make up the acceleration profile. It is widely recognized that jittering induces cybersickness [32].

For our experiment, if we picked the mean velocity (or mean optic flow) in the accelerated conditions and calculated the equivalent thresholds we found that they matched the thresholds for constant-velocity translations but were higher than the ones for the constant-velocity rotations. This observation is in contradiction with the sensory conflict theory since we would expect all the acceleration related thresholds to be lower than for the corresponding steady velocity conditions. This effect would be further exacerbated if we picked the maximum velocity observed in the scene.

Participants, when asked at the end of each run to describe their cybersickness onset symptoms, often remarked to have felt something just at the end of acceleration conditions. They also often remarked the shortness of the run and the wish to be exposed longer to the field to be more sure about what they experienced. It can also be observed in Figs. 6 and 7 that the trends between the forward and lateral cases and between roll and yaw were preserved for both the constant-velocity and the constant-acceleration conditions. These three observations led us to believe that the differences we observed in the detected thresholds was not caused by the acceleration but rather by the dynamics of vection perception. Previous studies have modeled the perception of angular and translational velocities with a low-pass filter with different time constants τ [30, 31]. Therefore we can express the perceived velocity as:

$$\omega_{vec} = \frac{1}{1+\tau_r s}\omega = \frac{1}{s(1+\tau_r s)}\alpha \tag{10}$$

$$V_{vec} = \frac{1}{1+\tau_t s}V = \frac{1}{s(1+\tau_t s)}a \tag{11}$$

where ω and V stand for the actual velocities of the scene while V_{vec} and ω_{vec} stand for the perceived ones. α and a stand for angular and linear acceleration. By requiring the perceived velocities to be equal to the threshold velocities found in the steady conditions allows us to estimate the time constant for the two different cases. We can find the time constants with:

$$\tau = \operatorname{argmin} L(\tau) = \operatorname{argmin} \frac{1}{2}\left((\omega_t - \omega_{vec}(\tau))^2 + (V_t - V_{vec}(\tau)^2\right) \tag{12}$$

Using the mean threshold value to find the time constant we obtained $\tau_t = 1.82$ s and $\tau_r = 3.78$ s. While this estimation is compatible with the literature, where τ_r is usually considered higher or equal to τ_t, it implies that participants did not fully perceive the angular velocity also for the constant-velocity cases. On the other hand, the confidence interval of the thresholds are rather large and contains values that lead to estimations compatible with the assumptions that participants perceived the actual angular velocity of the steady conditions at the end of the 5 seconds run.

D. Exposure Time

The exposure time is an important variable to consider while studying the onset of cybersickness. Cybersickness can be caused by sustained vection, which cannot be perceived instantly by humans. The literature seems to show that the onset time for vection varies depending on both the stimulus and the apparatus. Head mounted displays, projectors, and screens can lead to different onset times since they have different resolutions and levels of immersiveness, and they occupy a different portion of the total field of view. Different types of VR scenes and motion types can also lead to different onset times [33]. It can vary from just 1-2 seconds [30, 33] to 5 seconds [34] or even more [7]. There is the possibility that the current exposure times in this experiment were too short, in particular for the acceleration conditions. We chose such a short exposure time to minimize persistent symptoms of cybersickness and limit the total duration of the experiment. During test runs in the design phase of the experiment, the chosen exposure times where sufficient to elicit sensations of uneasiness, disorientation or vection.

E. Effect of Optic-Flow Density

The optic flow as defined from our model is directly proportional to the density of the particle field. By changing the density in the forward condition we aimed to understand the relation between the optic flow threshold and the actual amount of optic flow in the scene. Previous studies reported that an increase in the density of forward-moving "dots" or particles did not increase the vection or the motion illness felt by the participants [2]. Even though in our study we did not found a significant trend, there is suggestive evidence that the vection and onset of cybersickness symptoms depend on the density. This suggests that the perceived vection possibly has a non linear relationship with respect to the density.

At the same time, research has shown that enriching the virtual environment with details influences how fast cybersickness symptoms are developed and their intensity [35]. The richness of details translates into a higher amount of information that is processed by peripheral vision. Given our simplified scene, we can see the density of the particle field as a proxy for the richness of details of the scene. An alternative explanation for the apparent conflict of the findings resides in the role of presence. The richness of the details might not directly translate into higher perceived motion but rather in a higher level of presence, which seems to be positively correlated with cybersickness [10]. We fail therefore to verify hypothesis *H3* since no significant trend between the density and the perceived threshold was found.

F. Correlations between Conditions

We found that there is a general correlation between all conditions, which means that there is an underlying individual sensitivity to the onset of cybersickness. Understanding and measuring this sensitivity can be helpful for developers of VR applications to tune their motion controls to users. In particular, by looking at Fig. 10, rotational conditions correlate strongly and significantly with each other and they are clustered in the correlation matrix. The only exception is condition YA which seems to strongly correlate with conditions FA, LS, and FS.50. The other big cluster is defined by the transnational cases. Indeed, conditions FS, FA, LS, LS, FS.75, and FS.50 also strongly correlate with each other. Given the high variability in cybersickness onset thresholds between individuals, the best way to reduce cybersickness, while not compromising the VR experience, seems to be to tune or adapt the motion settings to each individual. This tuning can also make use of the strong correlation between conditions to reduce the number of test conditions to detect the user susceptibility to cybersickness.

G. Biometrics data

For each participant we measured skin conductivity and the electrocardiogram. In this study we found that only the onset of cybersickness is correlated with a significant increase in heart rate. Albeit significant, the effect size is rather small and probably not detectable if more confounding factors are introduced, like the presence of physical exercise. It is therefore likely that to have both a significant and a moderate increase in heart beat and skin conductivity, the participant should experience stronger symptoms of cybersickness.

H. Possible Confounding Factors

One of the main possible pitfalls of this experiment is the placebo effect. Participants were told to look for a set of symptoms, which can be very subtle. Nonetheless, given the nature of the experiment nothing could be done about the placebo effect. Another risk factor is the misunderstanding of the set of symptoms to look for. Since we are testing for the onset of cybersickness participants don't have to experience severe symptoms, for example, nausea is a sufficient but not necessary condition for the detection of the threshold. To minimize this risk, the list of symptoms to look for

was put on paper and read twice to the participants. It is also believed that while vection is a necessary condition for cybersickness it is not a sufficient one [3]. Furthermore, this whole research relies on the assumption that the thresholds for the onset of cybersickness is strongly correlated with the propensity of the participant to cybersickness. While there is evidence that the symptoms detected with this research are linked to cybersickness, no formal study has linked the onset of cybersickness with actual cybersickness.

VII. Conclusion

This paper was the first to determine velocity and acceleration thresholds for the onset of cybersickness. Participants were exposed in a virtual environment to moving particle fields. Four different optic-flow types were used: forward, lateral, roll and yaw, and two different motion types: constant velocity or acceleration. The optic flow of each condition was modeled and equalized across conditions to allow for the direct comparison of thresholds. In addition, the density of the particles was varied for the forward moving optic flow. Participants were exposed to the optic flow for only a few seconds at a time, after which they were asked if they felt uneasiness or symptoms associated with cybersickness. The threshold for the onset of cybersickness was found using a staircase procedure that controlled the speed or acceleration of the particle field.

Results indicated a significant difference in thresholds between the translational and rotational optic flow types. The thresholds were significantly lower for rotational optic flow. In addition, the motion profile (constant velocity or acceleration) had a clear influence on the thresholds. It is uncertain though how to compare the acceleration and velocity thresholds. Given the short exposure time, the transient dynamics of visual motion perception play a role in the detection of the acceleration thresholds. Rather than concluding that accelerations could lead to cybersickeness quicker, these transient dynamics could explain the observed differences between velocity and acceleration thresholds. Furthermore, it was found that the thresholds suggestively decreases with the density of the particles in the scene, which a proxy for the level of detail in a real scene. More research is needed to verify this trend. Finally, the different rotational or translational cases tend to strongly correlate with each other.

The results tend to confirm the theory of sensory conflict as an explanation for cybersickness. Rotations and possibly translational accelerations show lower thresholds compared to the rest of the conditions. The thresholds found in this paper can be used to design motion profiles in VR by controlling the speed and the presence of details in the peripheral vision. Furthermore, given the high variation in individuals' responses, motion settings should be personalized. This paper explored the onset of cybersickness and how different variables influence it. We recommend further research to validate that the optic flow threshold found for the onset of seasickness correlates with the severity of cybersickness symptoms and how quickly they appear. Furthermore, we encourage the use of these results to develop a technical solution for cybersickness.

VIII. Acknowledgements

The authors would like to thank the 18 participants who took part in the experiment. In addition, we thank Mike Feary, who allowed us to use the conventional fixed-base simulator and VR equipment of his lab. We also thank Bill Toscano and Fernando Espinosa for their collaboration and help with collecting and processing the biometrics.

References

[1] Fernandes, A. S., and Feiner, S. K., "Combating VR sickness through subtle dynamic field-of-view modification," *2016 IEEE Symposium on 3D User Interfaces (3DUI)*, 2016, pp. 201–210. doi:10.1109/3DUI.2016.7460053.

[2] Webb, N. A., and Griffin, M. J., "Eye movement, vection, and motion sickness with foveal and peripheral vision," *Aviation, Space, and Environmental Medicine*, Vol. 74, No. 6 Pt 1, 2003, pp. 622–625.

[3] Rebenitsch, L., and Owen, C., "Review on cybersickness in applications and visual displays," *Virtual Reality*, Vol. 20, 2016. doi:10.1007/s10055-016-0285-9.

[4] Bonato, F., Bubka, A., and Palmisano, S., "Combined pitch and roll and cybersickness in a virtual environment," *Aviation, Space, and Environmental Medicine*, Vol. 80, No. 11, 2009, pp. 941–945.

[5] "Oculus Rift Best Practices," 2015.

[6] Porcino, T. M., Clua, E., Trevisan, D., Vasconcelos, C. N., and Valente, L., "Minimizing cyber sickness in head mounted display systems: Design guidelines and applications," *2017 IEEE 5th International Conference on Serious Games and Applications for Health (SeGAH)*, 2017, pp. 1–6. doi:10.1109/SeGAH.2017.7939283.

[7] Bonato, F., Bubka, A., Palmisano, S., Phillip, D., and Moreno, G., "Vection Change Exacerbates Simulator Sickness in Virtual Environments," *Presence*, Vol. 17, 2008, pp. 283–292. doi:10.1162/pres.17.3.283.

[8] Rebenitsch, L., and Owen, C., "Review on cybersickness in applications and visual displays," *Virtual Reality*, Vol. 20, No. 2, 2016, pp. 101–125. doi:10.1007/s10055-016-0285-9, URL https://doi.org/10.1007/s10055-016-0285-9.

[9] Kennedy, R., Drexler, J., and Kennedy, R., "Research in visually induced motion sickness," *Applied ergonomics*, Vol. 41, 2010, pp. 494–503. doi:10.1016/j.apergo.2009.11.006.

[10] Weech, S., Kenny, S., and Barnett-Cowan, M., "Presence and Cybersickness in Virtual Reality Are Negatively Related: A Review," *Frontiers in Psychology*, Vol. 10, 2019, p. 158. doi:10.3389/fpsyg.2019.00158, URL https://www.frontiersin.org/article/10.3389/fpsyg.2019.00158.

[11] Davis, S., Nesbitt, K., and Nalivaiko, E., "A Systematic Review of Cybersickness," *Proceedings of the 2014 Conference on Interactive Entertainment - IE2014*, ACM Press, Newcastle, NSW, Australia, 2014, pp. 1–9. doi:10.1145/2677758.2677780, URL http://dl.acm.org/citation.cfm?doid=2677758.2677780.

[12] Nie, G., Liu, Y., and Wang, Y., "[POSTER] Prevention of Visually Induced Motion Sickness Based on Dynamic Real-Time Content-Aware Non-salient Area Blurring," *2017 IEEE International Symposium on Mixed and Augmented Reality (ISMAR-Adjunct)*, 2017, pp. 75–78. doi:10.1109/ISMAR-Adjunct.2017.35.

[13] Horn, B., and Schunck, B., "Determining Optical Flow," *Artificial Intelligence*, Vol. 17, 1981, pp. 185–203. doi:10.1016/0004-3702(81)90024-2.

[14] James J. Gibson; Leonard Carmichael, E. B. H. M., "The Perception of the Visual World," *Science*, Vol. 113, No. 2940, 1951, pp. 535–535. doi:10.1126/science.113.2940.535, URL https://science.sciencemag.org/content/113/2940/535.1.

[15] Kennedy, R. S., Lane, N. E., Berbaum, K. S., and Lilienthal, M. G., "Simulator Sickness Questionnaire: An Enhanced Method for Quantifying Simulator Sickness," *The International Journal of Aviation Psychology*, Vol. 3, No. 3, 1993, pp. 203–220. doi:10.1207/s15327108ijap0303_3, URL https://doi.org/10.1207/s15327108ijap0303_3.

[16] Wentink, M., Bos, J., Groen, E., and Hosman, R., "Development of the Motion Perception Toolbox," 2006. doi:10.2514/6.2006-6631.

[17] Cutting, J. E., Vishton, P. M., Flückiger, M., Baumberger, B., and Gerndt, J. D., "Heading and path information from retinal flow in naturalistic environments," *Perception & Psychophysics*, Vol. 59, No. 3, 1997, pp. 426–441. doi:10.3758/BF03211909, URL https://doi.org/10.3758/BF03211909.

[18] Warren, W., and Hannon, D., "Direction of self-motion is perceived from optical flow," *Nature*, Vol. 336, 1988, pp. 162–163.

[19] Lucas, B., and Kanade, T., "An Iterative Image Registration Technique with an Application to Stereo Vision (IJCAI)," 1981.

[20] Cornsweet, T. N., "The Staircase-Method in Psychophysics," *The American Journal of Psychology*, Vol. 75, No. 3, 1962, pp. 485–491. URL http://www.jstor.org/stable/1419876.

[21] Levitt, H., "Transformed Up-Down Methods in Psychoacoustics," *The Journal of the Acoustical Society of America*, Vol. 49, No. 2B, 1971, pp. 467–477. doi:10.1121/1.1912375, URL https://doi.org/10.1121/1.1912375.

[22] Kim, Y. Y., Kim, E. N., Park, M. J., Park, K. S., Ko, H. D., and Kim, H. T., "The Application of Biosignal Feedback for Reducing Cybersickness from Exposure to a Virtual Environment," *Presence: Teleoperators and Virtual Environments*, Vol. 17, No. 1, 2008, pp. 1–16. doi:10.1162/pres.17.1.1, URL https://doi.org/10.1162/pres.17.1.1.

[23] Warren, W., and Hannon, D., "Eye movements and optical flow," *Journal of the Optical Society of America. A, Optics and image science*, Vol. 7, 1990, pp. 160–9. doi:10.1364/JOSAA.7.000160.

[24] Kennedy, R. S. D., "Configural Scoring of Simulator Sickness, Cybersickness and Space Adaptation Syndrome: Similarities and Differences?" , Jan. 2001. URL https://ntrs.nasa.gov/search.jsp?R=20100033371.

[25] Mazloumi Gavgani, A., Nesbitt, K., Blackmore, K., and Nalivaiko, E., "Profiling subjective symptoms and autonomic changes associated with cybersickness," *Autonomic neuroscience : basic & clinical*, Vol. 203, 2016. doi:10.1016/j.autneu.2016.12.004.

[26] Rokach, L., and Maimon, O., *Clustering Methods*, Springer US, Boston, MA, 2005, pp. 321–352. doi:10.1007/0-387-25465-X_15, URL https://doi.org/10.1007/0-387-25465-X_15.

[27] Borst, A., and Euler, T., "Seeing Things in Motion: Models, Circuits, and Mechanisms," *Neuron*, Vol. 71, 2011, pp. 974–94. doi:10.1016/j.neuron.2011.08.031.

[28] Im, M., and Fried, S., "Directionally selective retinal ganglion cells suppress luminance responses during natural viewing," *Scientific Reports*, Vol. 6, 2016, p. 35708. doi:10.1038/srep35708.

[29] Werkhoven, P., Snippe, H., and Toet, A., "Visual processing of optic acceleration," *Vision research*, Vol. 32, 1993, pp. 2313–29. doi:10.1016/0042-6989(92)90095-Z.

[30] Wentink, M., Bos, J., Groen, E., and Hosman, R., "Development of the Motion Perception Toolbox," 2006. doi:10.2514/6.2006-6631.

[31] Bos, J., Hosman, R., and Bles, W., "Visual-Vestibular Interactions and Spatial (Dis)Orientation in Flight and Flight Simulation," 2002, p. 29.

[32] LaViola, J. J., Jr., "A Discussion of Cybersickness in Virtual Environments," *SIGCHI Bull.*, Vol. 32, No. 1, 2000, pp. 47–56. doi:10.1145/333329.333344, URL http://doi.acm.org/10.1145/333329.333344.

[33] Palmisano, S. A., and Riecke, B. E., "The search for instantaneous vection: An oscillating visual prime reduces vection onset latency," *PloS one*, 2018.

[34] Brandt Th., K. E., Dichgans J., "Differential effects of central versus peripheral vision on egocentric and exocentric motion perception," *Experimental Brain Research*, Vol. 16, 1973, pp. 476–491.

[35] Davis, S., Nesbitt, K., and Nalivaiko, E., "Comparing the onset of cybersickness using the Oculus Rift and two virtual roller coasters," *Proceedings of the 11th Australasian Conference on Interactive Entertainment (IE 2015)*, Vol. 27, 2015, p. 30.